Facile Syntheses of Surface-Functionalized Micelles and Shell Cross-Linked Nanoparticles

RACHEL K. O'REILLY,[1,2*] MAISIE J. JORALEMON,[1†] CRAIG J. HAWKER,[2,3] KAREN L. WOOLEY[1]

[1]Center for Materials Innovation and Department of Chemistry, Washington University, Saint Louis, Missouri 63130-4899

[2]IBM Almaden Research Center, San Jose, California 95120

[3]Materials Research Laboratory, University of California, Santa Barbara, California 93106

Received 23 December 2005; accepted 28 February 2006
DOI: 10.1002/pola.21602
Published online in Wiley InterScience (www.interscience.wiley.com).

ABSTRACT: Block copolymer micelles and shell cross-linked nanoparticles (SCKs) presenting Click-reactive functional groups on their surfaces were prepared using two separate synthetic strategies, each employing functionalized initiators for the controlled radical polymerization of acrylate and styrenic monomers to afford amphiphilic block copolymers bearing an alkynyl or azido group at the α-terminus. The first route for the synthesis of the azide-functionalized nanostructures was achieved via sequential nitroxide-mediated radical polymerization (NMP) of *tert*-butyl acrylate and styrene, originating from a benzylic chloride-functionalized initiator, followed by deprotection of the acrylic acids, supramolecular assembly of the block copolymer in water and conversion of the benzylic chloride to a benzylic azide. In contrast, the second strategy utilized an alkynyl-functionalized reversible addition fragmentation transfer (RAFT) agent directly for the RAFT-based sequential polymerization of tetrahydropyran acrylate and styrene, followed by selective cleavage of the tetrahydropyran esters to give the α-alkynyl-functionalized block copolymers. These Click-functionalized polymers, with the functionality located at the hydrophilic polymer termini, were then self-assembled using a mixed-micelle methodology to afford surface-functionalized "Clickable" micelles in aqueous solutions. The optimum degree of incorporation of the Click-functionalized polymers was investigated and determined to be *ca*. 25%, which allowed for the synthesis of well-defined surface-functionalized nanoparticles after cross-linking selectively throughout the shell layer using established amidation chemistry. Functionalization of the chain ends was shown to be an efficient process under standard Click conditions and the resulting functional groups revealed a more "solution-like" environment when compared to the functional group randomly inserted into the hydrophilic shell layer. J Polym Sci Part A: Polym Chem 44: 5203–5217, 2006
Keywords: block copolymers; core-shell polymers; functionalization of polymers; nanoparticles; reversible addition fragmentation chain transfer (RAFT)

INTRODUCTION

The solution-state self-assembly and covalent stabilization of block copolymers to give materials displaying a wide range of morphologies[1–5] have attracted considerable interest over the last decade, due to their unique structure and

**Present address:* The University Chemistry Laboratory, University of Cambridge, Lensfield Road, CB2 1EW, Cambridge, United Kingdom
†*Present address:* Department of Polymer Science and Engineering, University of Massachusetts, Conte Center for Polymer Research, Amherst, Massachusetts 01003, USA
Correspondence to: C. J. Hawker and K. L. Wooley (E-mail: hawker@mrl.ucsb.edu)
Journal of Polymer Science: Part A: Polymer Chemistry, Vol. 44, 5203–5217 (2006)

properties, which can incorporate features similar to core-shell nanoparticles, hydrogels, and dendritic macromolecules. These nanostructured materials have potential for use in a wide range of applications in materials science and biomedicine,[6–8] and the development of methodologies for their preparation[9–12] and functionalization[13–15] is an area of active research.

Although many techniques are available for the preparation of nanoparticles, perhaps the most versatile is the self-assembly of amphiphilic block copolymers in selective solvents, to afford polymer micelles[16–23] or vesicles.[24,25] These polymeric assemblies can then be stabilized through covalent cross-linking, in either the core[26,27] or shell[23,28] domains to afford stabilized amphiphilic nanoparticles with well-defined core-shell morphologies. By limiting the cross-links to the polymer chain segments that compose the micelle periphery, shell cross-linked nanoparticles (SCKs) can be formed, which consist of a hydrophobic core domain and a cross-linked hydrophilic shell layer.[29,30] Our interest is primarily focused on these amphiphilic nanostructures because of their analogy to biological constructs;[31] however, entirely hydrophobic,[32] hydrophilic,[21,33] zwitterionic,[34] or schizophrenic[35] shell cross-linked polymer assemblies have also been reported.

In analogy with lipoproteins,[36–39] shell cross-linked nanoparticles (SCKs) have been demonstrated to be biocompatible, stable,[40–42] and capable of hydrophobic guest sequestration and transport. Furthermore, there has been ever-growing interest in the bioconjugation of nanoparticles[43,44] to allow the attachment and surface presentation of ligands for complexation and coordination, in applications ranging from biometrics to targeted delivery and biodetection.[45–54] It has been reported that these SCK nanoparticles can be surface conjugated with mannose,[55] folate,[56,57] peptides,[58,59] antibodies,[60] and other moieties.[61–64] To date, two primary synthetic strategies for the introduction of surface accessible functional groups have been established and involve either use of a functionalized initiator species,[55,62] and thus a mixed-micelle strategy, or random functionalization in the shell layer postnanoparticle preparation.[56,65,66]

Each strategy has been demonstrated to afford nanoparticles with both surface- and bioavailable functional groups; however, the degree of control associated with randomly incorporating functional groups into the hydrophilic shell of SCKs is low and the efficiency of presenting these molecular recognition elements on the nanoparticle surface is unknown.[57,67–69] Similarly, a significant disadvantage of the functionalized initiator strategy is that complex synthetic routes are often required to obtain the desired functionality at the hydrophilic polymer chain end and a different initiator is required for each functional group. As a result, this strategy can be limited by synthetic challenges and possible incompatibility with the polymerization chemistry mandating complex protection strategies and further restricting the range of possible functional groups.

To broaden the range of surface functional groups and to maximize their presentation at the nanoparticle surface, a versatile approach involving a common functionalized initiator leading to surface-available chemical handles designed for facile attachment of desired moieties to the surface-functionalized micelle/nanoparticle was developed. The strategy employed was that of Click chemistry,[70] which has recently been demonstrated to be an extremely efficient and versatile method for the functionalization of biomolecules, surfaces, inorganic substrates, and polymers.[71–80] This strategy involves the synthesis of alkynyl- and azido-functionalized amphiphilic block copolymers, which can then be supramolecularly self-assembled using a mixed micelle methodology and cross-linked to afford Clickable nanoparticles. These nanoparticles have the potential to be transformed under Click conditions, using the complementary reagent, into a wide range of surface-functionalized micelles/nanoparticles while maximizing the presentation of the chain end functional groups.

RESULTS AND DISCUSSION

Azido Chain End-Functionalized Amphiphilic Block Copolymers

Initial investigations into the preparation of chain end-functionalized amphiphilic block copolymers involved the synthesis of azido-functionalized alkoxyamine initiators for utilization in nitroxide-mediated radical polymerization (NMP). On the basis of prior results,[81] the chloromethyl-functionalized initiator, 2,2,5-trimethyl-3-(1-(4′-chloromethyl)phenylethoxy)-4-phenyl-3-azahexane, was employed as a latent azido functionality, due to incompatibility of the azido functionality with the chemistry, employed for ester deprotection (the

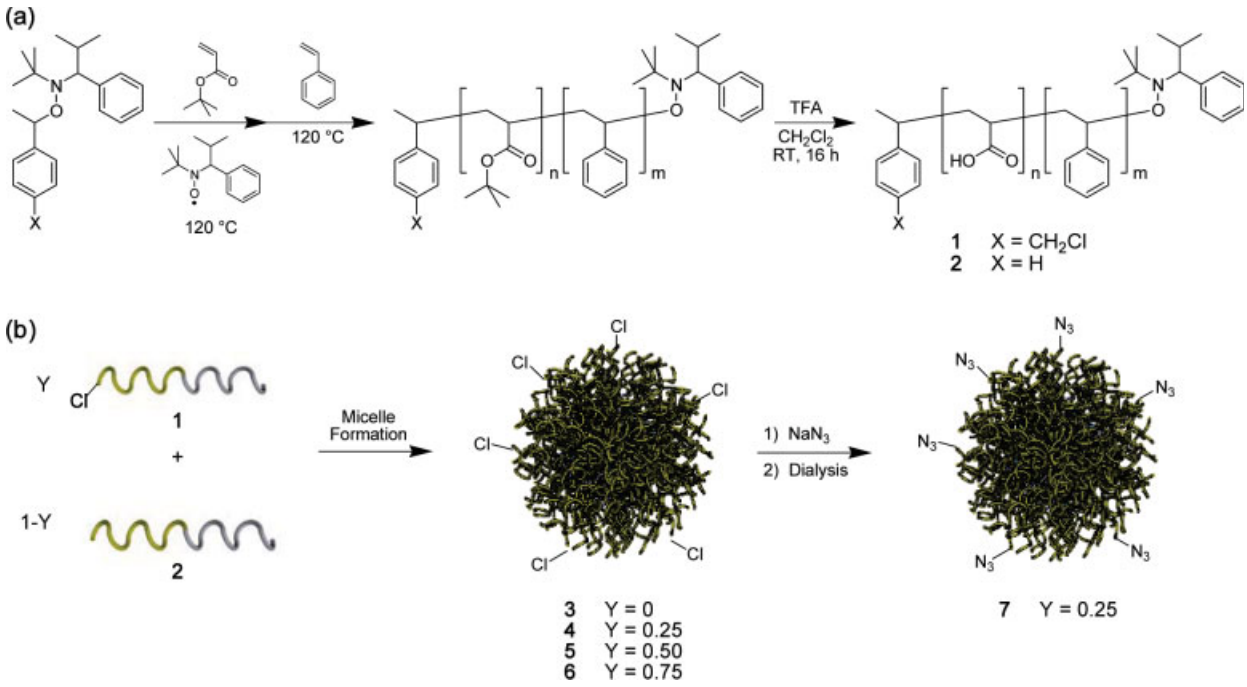

Scheme 1. (a) Syntheses of amphiphilic block copolymers **1** and **2**; (b) Mixed micelle strategy to assemble micelles **3**–**6** and subsequent chemical modification of **4** to afford azide-functionalized micelle **7**. [Color figure can be viewed in the online issue, which is available at www.interscience.wiley.com.]

final step to produce the amphiphilic block copolymer). The synthesis of the chloromethyl-substituted alkoxyamine NMP initiator and the subsequent polymerization of *tert*-butyl acrylate (*t*-BuA) followed by styrene (St) has been previously reported.[82] Following similar experimental conditions, the $ClCH_2P$*t*-BuA_{60}-*b*-PS_{135} block copolymer with a chloromethyl moiety at the acrylate chain end was isolated ($M_{n,GPC}$ = 22,500 g/mol, M_w/M_n = 1.18, $M_{n,NMR}$ = 22,800 g/mol). The *tert*-butyl ester groups in the polymer were then removed by treatment with trifluoroacetic acid (TFA) using established chemistries (Scheme 1a), which afforded the amphiphilic block copolymer $ClCH_2$ PAA_{60}-*b*-PS_{135}, **1**, with the latent azido group at the hydrophilic chain terminus ($M_{n,NMR}$ = 18,900 g/mol). Using a similar strategy and the nonfunctionalized alkoxyamine initiator, 2,2,5-trimethyl-3-(1-phenylethoxy)-4-phenyl-3-azahexane, PAA_{65}-*b*-PS_{135}, **2**, ($M_{n,NMR}$ = 19,400 g/mol) was also synthesized and was then assembled together with **1** into mixed block copolymer micelles. The block copolymers were designed to be composed of similar hydrophobic and hydrophilic block segment compositions and lengths to provide for a random incorporation and uniform distribution of the mixed polymer chains throughout the micelles.

The fidelity of this mixed micelle strategy was investigated by exploring a range of functionalized to nonfunctionalized polymer ratios and determining the effects of these ratios on the formation of well-defined micelles (Scheme 1b). It had been demonstrated previously that a high ratio of functionalized block copolymers led to ill-defined and aggregated micelles, as observed by dynamic light scattering (DLS) analysis.[62] Micelles **3**–**6** were, therefore, prepared by dissolution of various ratios of the block copolymers **1** and **2** in THF (a good solvent for both the PS and PAA segments), followed by the gradual addition of an equal volume of water (a nonsolvent for PS) to induce micelle formation. Following extensive dialysis of the THF/water mixture into Nanopure water, stabilization of the micellar assemblies was established and a series of micelles and mixed polymer micelles, **3**–**6**, was formed, with a theoretical chloromethyl chain end incorporation of 0, 25, 50, and 100%, respectively.

The hydrodynamic diameters of the micelles, **3**–**6**, were determined by DLS (Table 1). Table 1 indicates that the optimum degree of surface functionalization in this micelle system is 25%; for higher degrees of functionalization, signifi-

Table 1. Hydrodynamic Diameters of micelles **3–6** Measured by DLS Analysis and Average Diameters Measured by TEM Analysis

		DLS[a]			
Micelle	Y	D_i (nm)	D_v (nm)	D_n (nm)	D_{av} (nm) [TEM[b]]
3	0	47 ± 1	46 ± 2	44 ± 4	32 ± 3
4	0.25	51 ± 2	48 ± 2	47 ± 3	35 ± 4
5	0.50	67 ± 15	48 ± 10	37 ± 7	30 ± 8
6	1.0	78 ± 16	69 ± 9	49 ± 8	43 ± 9

[a] Number–averaged hydrodynamic diameters of micelles in aqueous solution by dynamic light scattering. D_i, intensity averaged diameter; D_v, volume average diameter; D_n, number averaged diameter.

[b] Average diameters of micelles were measured by TEM from the values for about 150 particles.

cant amounts of aggregation were observed with the polydispersity of the micelles (D_v/D_n) ranging from 1.30 to 1.40. Table 1 illustrates that the incorporation of around 25% of chloromethyl-terminated polymers in micelle **4** does not have a significant effect on the hydrodynamic diameter or polydispersity as determined by DLS ($D_v/D_n = 1.02$) compared to the nonfunctionalized micelle **3** ($D_v/D_n = 1.05$). For the micelles with high degrees of surface functionalization, **5** and **6**, a significant degree (*ca*. 10%) of larger irregular aggregates of diameter *ca*. 150 nm were observed by DLS measurements. The micelles **3–6** were also analyzed using transmission electron microscopy (TEM) analysis and representative images are shown in Figure 1, which fully support the DLS results.

Having established an optimum level of chloromethyl group incorporation, the 25% functionalized micelles **4** were initially allowed to undergo reaction with excess sodium azide for 2 days at room temperature, followed by dialysis for 4 days into Nanopure water to remove excess sodium azide and other sodium salts. It was considered important to functionalize the micelles prior to SCK nanoparticle formation because of the possibility of the chloromethyl group to undergo reaction with the diamine cross-linking agent during covalent stabilization. The azido-terminated micelle, **7**, was analyzed by DLS, which indicated that the functional group transformation at the micellar chain ends did not affect the size or distribution of the micelles (*cf.* D_n (**4**) = 47 ± 3 nm vs. D_h (**7**) = 49 ± 3 nm). The conversion of the chloromethyl functionality to an azidomethyl group was confirmed by infrared (IR) and NMR spectroscopy, each performed upon a lyophilized aliquot of **7**. A comparison of the IR spectrum of **4** *versus* **7** highlighted the introduction of the strong azido absorbance at *ca.* 2100 cm^{-1} in micelle **7**. NMR analysis, upon a sample of the lyophilized material having been resuspended into D_2O, allowed for the extent of chloromethyl to azidomethyl conversion to be determined by using the methylene protons as a diagnostic handle. The disappearance of the methylene protons resonating at 4.45 ppm in **4**, attributable to the chloromethyl end group, and appearance of a new resonance upfield (4.65 ppm in **7**), attributable to the protons of the azidomethyl functionality, suggested the successful incorporation of the azido groups into the micelle.

Alkynyl Chain End-Functionalized Amphiphilic Block Copolymers

The block copolymer micelles, **8**, and SCKs, **9**, bearing alkynyl surface groups were prepared directly from α-alkynyl-functionalized amphiphilic block copolymers, without the use of a latent functionality as had been done for the azido-functionalized materials. To overcome the incompatibility of the alkynyl functionality with the reaction conditions

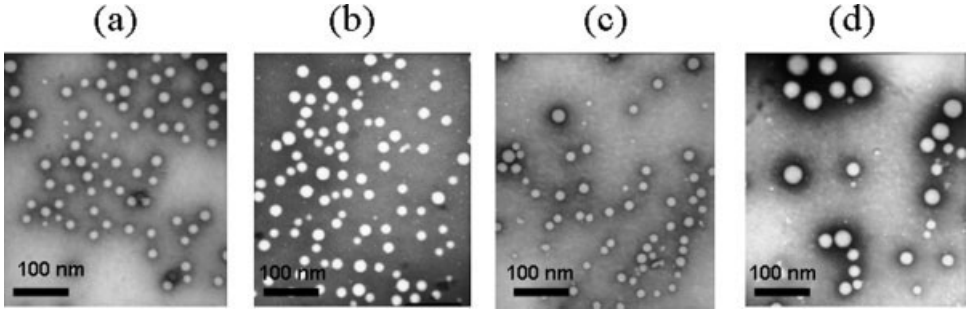

Figure 1. TEM images of micelles: (a) **3**, (b) **4**, (c) **5,** and (d) **6**. Samples were stained with PTA and drop deposited onto a carbon-coated copper grid.

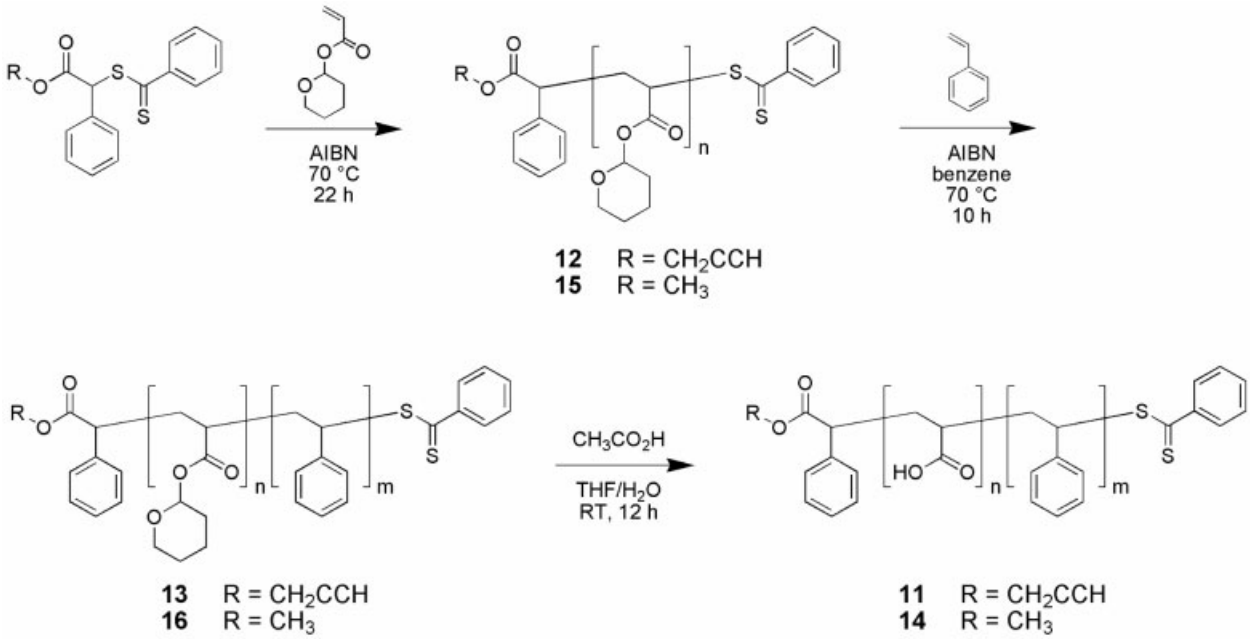

Scheme 2. Syntheses of chain end alkynyl-functionalized block copolymers **13** and **11** and nonfunctionalized block copolymers **16** and **14**.

required for acidolysis of the *tert*-butyl esters, we chose to employ tetrahydropyran (THP) as an alternate protecting group. Unfortunately the polymerization of tetrahydropyran acrylate (THPA) under NMP conditions was not successful, due to uncontrolled cleavage of the THP group at the elevated temperatures of the polymerization system, which resulted in poorly defined polymers. Using the THP[83] protecting group together with the milder polymerization conditions of reversible addition fragmentation transfer (RAFT),[84] the incorporation of an alkyne into the hydrophilic chain terminus proceeded smoothly from the alkynyl-RAFT agent, **10**.[85] As illustrated in Scheme 2, preparation of the alkynyl chain end-functionalized amphiphilic diblock copolymer **11**, HC≡CPAA$_{70}$-*b*-PS$_{135}$, began by the sequential RAFT of THPA to give the THPA homopolymer macroRAFT agent **12** ($M_{n,GPC}$ = 11,900 g/mol, M_w/M_n = 1.12, $M_{n,NMR}$ = 11,000 g/mol), followed by St to give diblock copolymer **13** ($M_{n,GPC}$ = 26,100 g/mol, M_w/M_n = 1.15, $M_{n,NMR}$ = 25,300 g/mol). Cleavage of the THP ester upon reaction with acetic acid in a mixture of tetrahydrofuran and water afforded the amphiphilic block copolymer **11** (Scheme 2).[86] Cleavage of the THP ester was confirmed using IR spectroscopy (observed bathochromic shift of carbonyl stretch from 1727 to 1705 cm^{-1}). In addition, the presence of the alkynyl functionality in the amphiphilic block copolymer, **11**, was confirmed by the characteristic absorbances at 3296 and 2120 cm^{-1}. ^{1}H NMR spectroscopy confirmed the disappearance of the THP acetal proton resonating at 5.9–6.0 ppm and also the presence of the carboxylic acid groups was confirmed by the appearance of a broad resonance at *ca.* 12.5 ppm. The conversion of the THP esters into carboxylic acid groups was also observed by differential scanning calorimetry (DSC) analyses, from which an increase in the glass transition temperature (T_g) value was observed upon transformation of the esters to acrylic acid residues, while the T_g for the PS domains remained constant (T_g (**13**) = 48 and 103 °C and T_g (**11**) = 131 and 99 °C). Finally integration of the unique acetylenic and methylene resonances for **11**, **12**, and **13** allowed the molecular weight to be determined and comparison of this value with the experimentally determined GPC values (assuming a single propargyl chain end) showed essentially complete chain end fidelity and no loss of acetylenic groups during polymerization or deprotection.

To allow for the greatest degree of structural similarity, a nonfunctionalized amphiphilic block copolymer, **14**, was also synthesized using RAFT polymerization and deprotection. Polymerization of THPA in the presence of the nonfunctional-

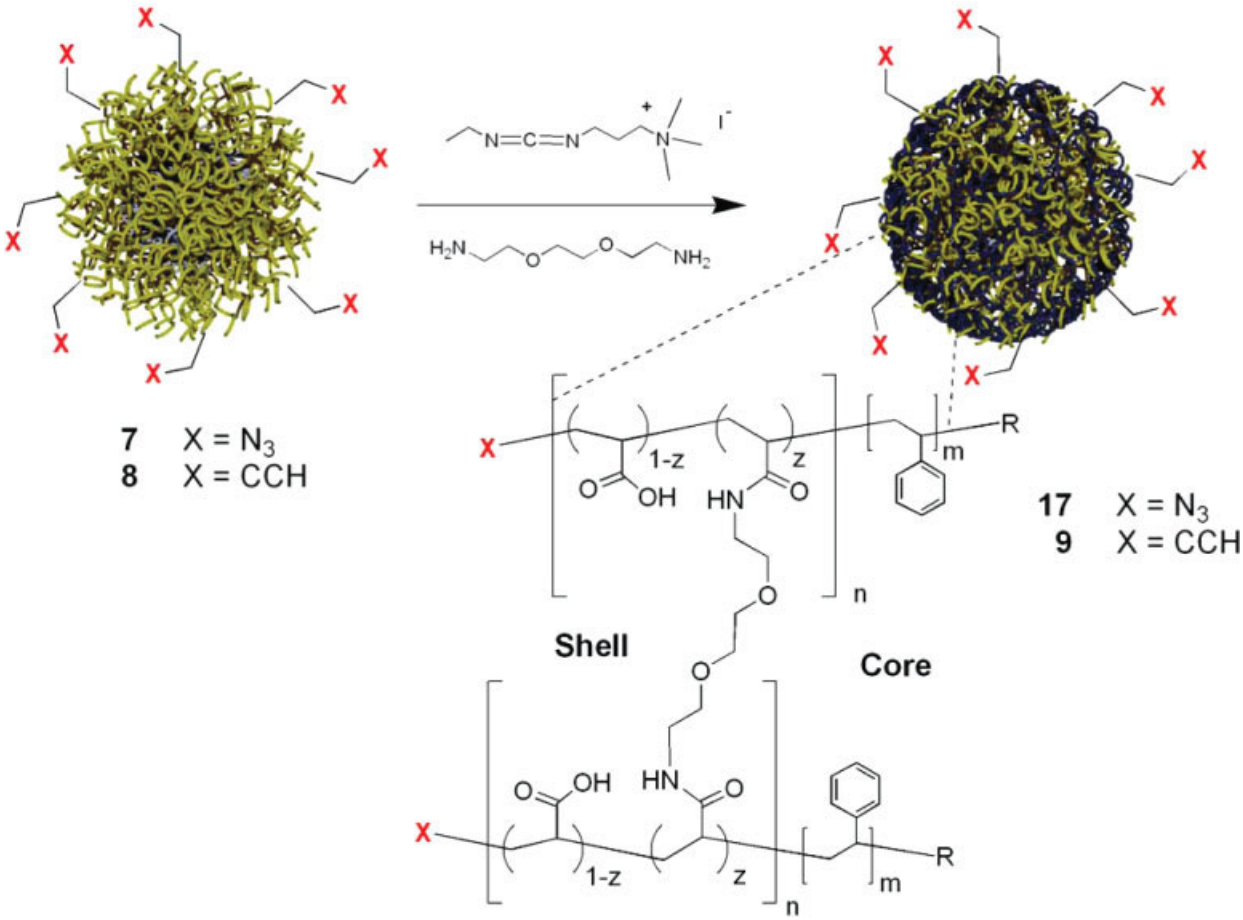

Scheme 3. Cross-linking of the hydrophilic shell in micelles **7** and **8** to afford SCK nanoparticles **17** and **9**, respectively.

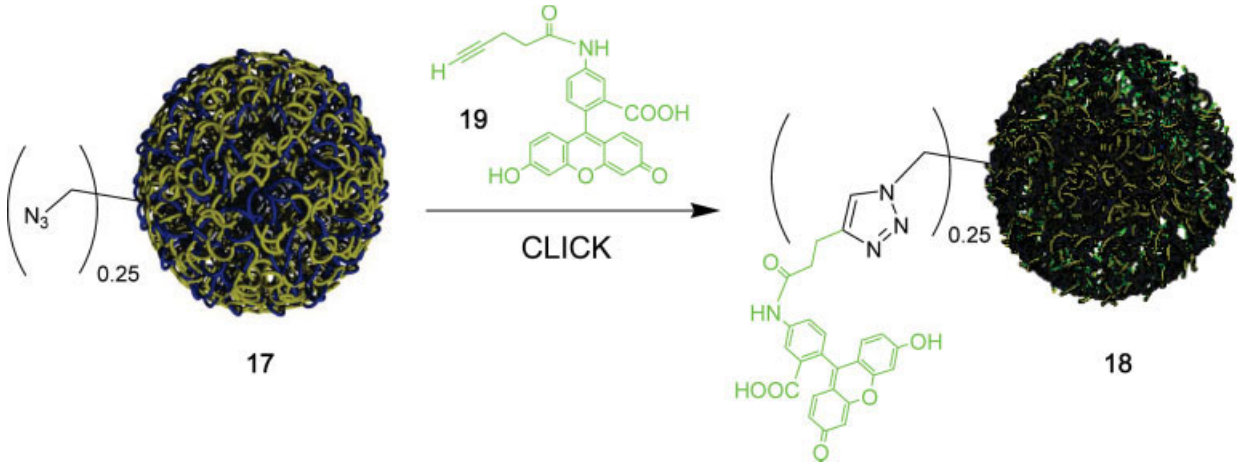

Scheme 4. Fluorescent labeling of surface Click-readied nanoparticle, **17**. Reagents and conditions for "Click" included $CuSO_4 \cdot 5H_2O$ (0.25 equiv), Na ascorbate (5 wt % solution in water, 0.50 equiv), alkynyl dye (1.11 equiv to azido functionality), RT, 2 days, followed by dialysis against pH 7.3 phosphate-buffered saline, 10 days.

Table 2. Comparison of Characterization Data for SCKs **17** and **9** and Click SCK, **18**

		AFM		
Particle	D_n[a] (nm) [DLS]	D_{av}[c] (nm)	H_{av}[c] (nm)	D_{av}[b] (nm) [TEM]
17	44 ± 3	104 ± 16	4.8 ± 1.2	34 ± 4
9	43 ± 4	117 ± 18	2.4 ± 0.4	32 ± 3
18	34 ± 4	126 ± 14	8.9 ± 2.2	37 ± 5

[a] Number-averaged hydrodynamic diameters of SCKs in aqueous solution by dynamic light scattering.
[b] Average diameters of SCKs were measured by TEM, from the values for about 150 particles.
[c] Average heights and diameters of SCKs were measured by tapping-mode AFM, averaged from the values for about 150 particles.

ized methyl carboxylate RAFT agent gave **15** ($M_{n,GPC}$ = 11,300 g/mol, M_w/M_n = 1.11, $M_{n,NMR}$ = 10,800 g/mol), and then extension with St produced the diblock copolymer **16** ($M_{n,GPC}$ = 25,200 g/mol, M_w/M_n = 1.16, $M_{n,NMR}$ = 24,100 g/mol). Following deprotection and dialysis the non-functionalized RAFT amphiphilic block copolymer, **14** was isolated for utilization with **11** to form mixed micelles.

Mixed micelles composed of the amphiphilic block copolymers **11** and **14** (in ratio 1:3) were then prepared as described for the chloro/azido chain end derivatives, to afford micelle **8**, with a theoretical surface functionalization of *ca.* 25%. At 25%, the alkynyl chain end-functionalized micelle was found to have a hydrodynamic diameter of 49 ± 4 nm, as determined by DLS analysis, and an average diameter of 37 ± 3 nm by TEM analysis. In addition, the presence of the alkynyl functionality in the micelle was confirmed by lyophilization of an aliquot, followed by IR spectroscopy, from which absorbances were observed at 3299 and 2121 cm^{-1}.

Cross-Linking of Click-Functionalized Micelles

Covalent stabilization of both Click-functionalized micellar systems was then accomplished by cross-linking of the hydrophilic shell layer of the azido- and alkynyl-functionalized micelles, **7** and **8**, using well-established amidation chemistry, to afford SCK nanoparticles, **17** and **9**, respectively, (Scheme 3). Each of the micelles were cross-linked at a calculated mean cross-linking density of 50%, based on the stoichiometry of amine functional groups of the diamine cross-linker to the carboxylic acid groups from the PAA-*b*-PS block copolymers. The amide bond formation was confirmed via IR spectroscopy by the introduction of amide bands at *ca.* 1640 and 1560 cm^{-1} and the size and shape of the SCKs were measured in the solid state by AFM and TEM, and in solution using DLS (*cf.* D_n (**4**) = 47 ± 3 nm vs. D_n (**7**) = 49 ± 3 nm *versus* D_n (**17**) = 44 ± 3 nm) (Table 2; Fig. 2). The larger diameter values (D_{av}) obtained from AFM measurements in comparison to those from TEM indicate significant deformation from the spherical

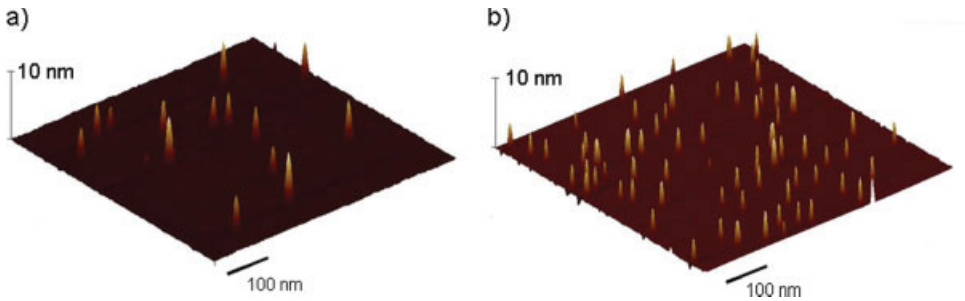

Figure 2. Representative tapping-mode AFM images of nanoparticles (a) **17** and (b) **9**. Samples were prepared by drop deposition onto freshly cleaved mica and allowed to dry under ambient conditions. [Color figure can be viewed in the online issue, which is available at www.interscience.wiley.com.]

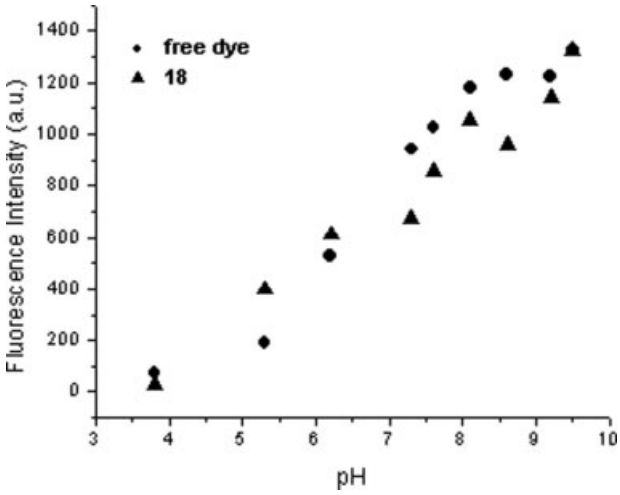

Figure 3. Comparison plots of fluorescence emission intensities from nanoparticle **18** (▲) and free alkynyl dye (●) (at λ_{em} = 517 nm) against pH. Each sample solution was prepared independently from a stock solution (*ca*. 0.28 mg/mL for nanoparticles) to ensure the same molar concentration of fluorescein units.

shape observed in solution, occurred upon absorption onto the hydrophilic mica AFM surface, as opposed to the hydrophobic carbon surface, the substrate for TEM characterization. As the lateral sizes of the particles (D_{av}) by AFM analysis are distorted due to the finite size of the AFM tip, particle diameters were measured by TEM analysis and found to correspond to those obtained for the corresponding micelle derivatives.

To confirm the presence and chemical availability of the alkyne and azide groups at the chain ends of the nanoparticles, a functionalization reaction was performed in which an azide- or alkyne-functionalized fluorescein dye, **19**, respectively, was allowed to undergo reaction under aqueous Click conditions. For example, reaction with the azido-functionalized nanoparticle **17** (Scheme 4) afforded the fluorescently labeled nanoparticle, **18** (Table 2). The presence and environment of the fluorescent dye at the chain ends of the nanoparticle was investigated using pH dependent fluorescence experiments with the free dye in solution serving as a control. Unlike the previously reported case when the dye was attached throughout the nanoparticle shell and, thus, was shielded by the carboxylic acid shell,[81] the pH dependent fluorescence spectra of **18** were very similar to the spectrum reported for the free dye in solution (Fig. 3). This result is significant, as it shows that dye attachment at the chain end (surface) of the nanoparticle leads to a more solution-like environment than the traditional strategy of random incorporation of the functionality throughout the hydrophilic shell, where it is sterically and electronically shielded by the poly(acrylic acid) chains. Confirmation that the fluorescein groups were covalently attached to the nanoparticles and not physisorbed was obtained by analytical ultracentifugation (AU) experiments, which clearly indicated that all of the dye was bound to the nanoparticle (Fig. 4). Analogous experiments were performed with the alkyne-functionalized nanoparticle, **9**, and the corresponding azido-substituted fluorescein dye and after exhaustive dialysis, UV–vis analysis indicated the attachment of the dye moiety with the same efficiency as for **18**.[91]

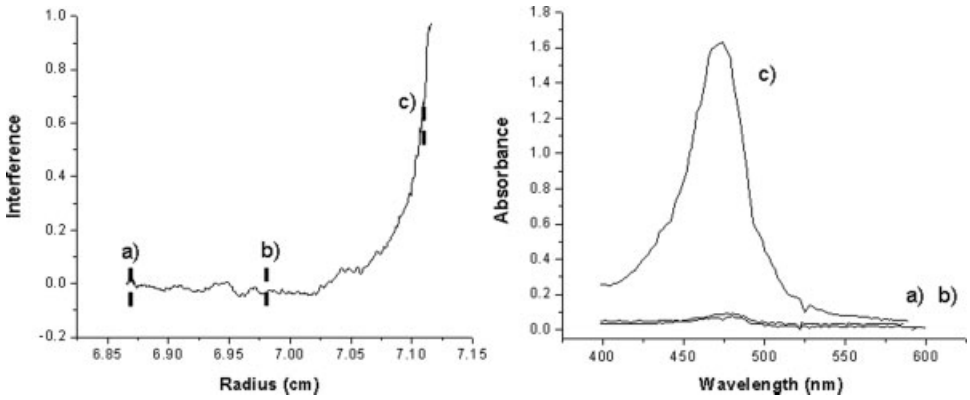

Figure 4. Sedimentation equilibrium profile (5000 rpm) collected using an interferometry detector for the nanoparticle **18** (left panel) and corresponding absorption spectra, recorded at different radial positions (right panel) across the sedimentation equilibrium profile: (a) top, (b) middle, and (c) bottom.

CONCLUSIONS

A general strategy for the synthesis of chain end-functionalized polymer micelles and nanoparticles has been developed based on functionalized alkoxyamine initiators and RAFT agents. Because of the high selectively and orthogonality of Click chemistry, this platform approach allows the resulting azide and alkyne functional groups to be transformed into a plethora of other functionalized nanostructures and the mild, aqueous reaction conditions permit reactive biological systems to be introduced readily. This last feature is difficult to accomplish using traditional techniques. The results presented herein also suggest that functionalities introduced selectively at the chain ends possess a more "solution-like" nanoenvironment compared to random distribution throughout the hydrophilic shell layer. Further work is currently underway to determine if this "solution-like" environment leads to enhanced bio- and chemical availability.

EXPERIMENTAL

Measurements

Hydrodynamic diameters (D_h) and size distributions for the micelles and SCK nanoparticles in aqueous solutions were determined by DLS. The DLS instrumentation consisted of a Brookhaven Instruments (Worcestershire, UK) system, including a model BI-200SM goniometer, a model BI-9000AT digital correlator, a model EMI-9865 photomultiplier, and a model 95-2 Ar ion laser (Lexel, Farmindale, NY) operated at 514.5 nm. Measurements were made at 20 ± 1 °C. Prior to analysis, solutions were centrifuged in a model 5414 microfuge (Brinkman Instruments, Westbury, NY) for 4 min to remove dust particles. Scattered light was collected at a fixed angle of 90 °C. The digital correlator was operated with 522 ratio spaced channels, and initial delay of 0.1 μs, a final delay of 5.0 μs, and a duration of 15 min. A photomulitplier aperture of 200 μm was used, and the incident laser intensity was adjusted to obtain a photon counting of between, 200 and 300 kcp s. Only measurements in which the measured and calculated baselines of the intensity autocorrelation function agreed to within 0.1% were used to calculate particle size. The calculations of the particle size distributions and distribution averages were performed with the ISDA software package (Brookhaven Instruments), which employed single-exponential fitting, cumulants analysis, non-negatively constrained least-squares and CONTIN particle size distribution analysis routines. All determinations were made in triplicate.

The height measurements and distributions for the nanoparticles were determined by tapping-mode AFM under ambient conditions in air. The AFM instrumentation consisted of a Nanoscope III BioScope system (Digital Instruments, Veeco Metrology Group, Santa Barbara, CA) and standard silicon tips (type, OTESPA-70; L, 160 μm; normal spring constant, 50 N/m; resonance frequency, 246–282 kHz). The sample solutions were prepared for AFM analysis by dilution (typical concentrations *ca*. 0.002 mg/mL) and deposition of a drop (2 μL) onto freshly cleaved mica and allowed to dry freely in air. The number–average particle heights (H_{av}) and diameter (D_{av}) values and standard deviations were generated from the sectional analysis of 150 particles from at least five different analysis regions.

TEM samples were diluted in water (9:1) and further diluted with a 1 wt % phosphotungstic acid (PTA) stain (1:1). Carbon grids were prepared by oxygen plasma treatment to increase the surface hydrophilicity. Micrographs were collected at 100,000× magnification and calibrated using a 41 nm polyacrylamide bead from National Institute of Standards and Technology. Histograms of number–average particle diameters (D_{av}) and standard deviations were generated from the analysis of a minimum of 150 particles from at least three different micrographs.

Sedimentation equilibrium experiments were conducted on a Beckman Instruments (Fullerton, CA) model Optima XL-I analytical ultracentrifuge fitted with a model An60-Ti four-hole rotor, and Epon charcoal-filled, six-channel centerpiece sample cells with either matched quartz windows. Data were recorded using the instrument's Rayleigh interfometric (refractive index) detection optics at 20 °C and 5000 rpm, with a centrifugation time of 2 days to reach sedimentation equilibrium. The solution volume was 110 μL, and the optical path length was 12 mm. Interference scans were obtained after sedimentation equilibrium had been reached, and then using this profile various radial positions in the cell (designated top, middle, and bottom) were identified and scanned using the UV–vis detection optics in the 400–600 nm region.

Nuclear magnetic resonance (^{1}H) was performed on a Bruker AVANCE 400 FTNMR spectrometer using deuterated solvents. Gel permeation chromatography was performed in THF on a Waters chromatograph equipped with four 5-μm Waters columns (300 $\times$ 7.7 mm^2) connected in series with increasing pore size (100, 1000, 10,000, and 1000,000 Å). Waters 410 differential refractometer index and 996 photodiode array detectors were employed. The molecular weights of the polymers were calculated relative to linear polystyrene standards. The modulated DSC measurements were performed with a TA Instruments, DSC 2920, and with a ramp rate of 4°/min. The glass-transition temperatures (T_g) were taken as the midpoint of the inflection tangent, upon the third heating scan. IR spectra were obtained on PerkinElmer Spectrum BX FTIR system using either diffuse reflectance sampling accessories or drop deposition onto NaCl plates.

Materials

tert-Butyl acrylate (*t*-BuA) and styrene (St) were purified by vacuum distillation from CaH_2 and then stored under N_2 at –15 °C. Dichloromethane (CH_2Cl_2) was dried by prolonged heating at reflux over CaH_2. All other materials were used as received from Sigma–Aldrich Company. Supor 25 mm 0.1 μm Spectra/Por Membrane tubes (molecular weight cut-off (MWCO) 6–8 kDa, Spectrum Medical Industries, Laguna Hills, CA) were used for dialysis. Stirred Ultrafiltration cell and Ultrafiltration Membrane Filter Discs (NMWL 10 kDa, Millipore, Bedford, MA) were used for concentration and dialysis of nanoparticle solutions. The following materials were synthesized according to literature methods: 2,2,5-trimethyl-3-(1-phenylethoxy)-4-phenyl-3-azahexane,[82] 2,2,5-trimethyl-3-(1-(4′-chloromethyl) phenylethoxy)-4-phenyl-3-azahexane,[82] 2,2,5-trimethyl-4-phenyl-3-azahexane-3-nitroxide,[82] THPA,[83] alkynyl fluorescein dye,[87,88] *S*-methoxycarbonylphenylmethyl dithiobenzoate,[89] and *S*-propargyloxycarbonylphenylmethyl dithiobenzoate.[85] The polymers P*t*-BuA$_{65}$-*b*-PS$_{135}$ ($M_{n,GPC}$ = 22,800 g/mol, M_w/M_n = 1.19) and ClCH$_2$P*t*-BuA$_{65}$-*b*-PS$_{135}$ ($M_{n,GPC}$ = 22,500 g/mol, M_w/M_n = 1.18) were synthesized using NMP as reported in the literature.[81] Readers are encouraged to consult the following literature reference prior to working with azido compounds.[90]

General Preparation of PAA$_n$-b-PS$_m$ Diblock Copolymers 1 and 2

To a 100-mL, round-bottom flask equipped with a stir bar was added P*t*-BuA$_{65}$-*b*-PS$_{135}$ ($M_{n,GPC}$ = 22,800 g/mol, M_w/M_n = 1.19; 1.0 g, 2.9 mmol of *t*-butyl ester), followed by dry dichloromethane (5.0 mL). The mixture was allowed to stir for 30 min to dissolve the polymer and then cooled to 0 °C. Trifluoroacetic acid (3.25 g, 28.5 mmol, 10.0 equiv to the *t*-butyl ester) was then added at 0 °C and the mixture allowed to stir overnight at RT. The dichloromethane and excess TFA were then removed at RT by passing air through the flask overnight. The resultant powdery off white solid was dried under vacuum to afford PAA$_{65}$-*b*-PS$_{135}$, **2** (0.79 g, 93% yield). The polymers were dissolved in THF (20 mL) and water (20 mL), transferred to presoaked dialysis membrane tubes (MWCO *ca.* 6–8 kDa), and dialyzed against deionized water for 4 days to obtain pure polymer. Lyophilization gave **2** as a white solid. DSC: $(T_g)_{PAA}$ = 131 °C, $(T_g)_{PS}$ = 99 °C.

IR: 3500–2800, 1941, 1875, 1701, 1601, 1585, 1490, 1450, 1235, 1170, 1117, 1068, 1031, 909, 878, 810, 755, 698, 539 cm^{-1}. ^{1}H NMR (DMSO-d_6, ppm, δ): 13.3–11.8 (br, COO*H*), 7.3–6.2 (m, 5Ar—*H*), 2.1–1.1 (br, C*H* and C*H*$_2$ of polymer backbone).

As described for **2** except ClCH$_2$P*t*-BuA$_{60}$-*b*-PS$_{135}$ was utilized to afford **1**, ClCH$_2$PAA$_{60}$-*b*-PS$_{135}$ (0.78 g, 95% yield): DSC: $(T_g)_{PAA}$ = 134 °C, $(T_g)_{PS}$ = 100 °C.

IR 3550–2850, 1785, 1710, 1487, 1454, 1266, 1217, 1168, 888, 761, 699 cm^{-1}. ^{1}H NMR (DMSO-d$_6$, ppm, δ): 12.7–11.9 (br, COO*H*), 7.3–6.3 (m, 5Ar—*H*), 4.5–4.4 (br, C*H*$_2$Cl), 2.2–1.2 (br, C*H* and C*H*$_2$ of polymer backbone).

Mixed Micelle Strategy for the Assembly of Micelles 3–6

A round-bottom flask equipped with a stir bar was charged with PAA$_{65}$-*b*-PS$_{135}$, **1** ($M_{n,NMR}$ = 19,400 g/mol) and ClCH$_2$PAA$_{60}$-*b*-PS$_{135}$, **2**, ($M_{n,NMR}$ = 18,900 g/mol) in various ratios, THF (1 mg/mL) was added, and the solution was allowed to stir at room temperature for 30 min to ensure the mixture was homogenous. Deionized water (1 mg/mL) was added via a metering pump at the rate of 20 mL/h. After all the water had been added, the bluish micelle solution was transferred to presoaked dialysis membrane tubes (MWCO *ca.* 6–8 kDa), and dialyzed against deionized water

for 4 days. **3** consists of 100% block copolymer **1**; D_h (DLS) = 44 ± 4 nm; D_{av} (TEM): 32 ± 3 nm; DSC: $(T_g)_{PAA}$ = 135 °C, $(T_g)_{PS}$ = 99 °C. **4** consists of 75% block copolymer **1**, 25% block copolymer **2**; D_h (DLS) = 47 ± 3 nm; D_{av} (TEM): 35 ± 4 nm; DSC: $(T_g)_{PAA}$ = 137 °C, $(T_g)_{PS}$ = 97 °C. **5** consists of 50% block copolymer **1**, 50% block copolymer **2**; D_h (DLS) = 37 ± 7 nm; D_{av} (TEM): 30 ± 8 nm DSC: $(T_g)_{PAA}$ = 140 °C, $(T_g)_{PS}$ = 96 °C. **6** consists of 100% block copolymer **2**; D_h (DLS) = 49 ± 8 nm; D_{av} (TEM): 43 ± 9 nm; DSC: $(T_g)_{PAA}$ = 136 °C, $(T_g)_{PS}$ = 100 °C.

Preparation of 25% Azide Surface-Functionalized Micelle, 7

To a stirred solution of micelle **4** (800 mL, 0.29 mg/mL, 0.003 mmol of chloromethyl groups) in a round-bottom flask, equipped with a stirrer bar, was added NaN_3 (0.001 g, 0.016 mmol, 5.0 equiv to chloro groups) dissolved in H_2O (1 mL). The reaction mixture was allowed to stir at RT for 3 days, transferred to presoaked dialysis membrane tubes (MWCO *ca.* 6–8 kDa), and dialyzed against deionized water for 4 days to remove the excess NaN_3 and sodium salts and to afford a polymer concentration of *ca.* 0.29 mg/mL. D_h (DLS) = 49 ± 3 nm; D_{av} (TEM): 36 ± 3 nm. Lyophilization gave a solid sample of **7** as a white solid. DSC: $(T_g)_{PAA}$ = 140 °C, $(T_g)_{PS}$ = 101 °C.

IR: 3610–2500, 2099, 1785, 1710, 1668, 1545, 1494, 1452, 1248, 1168, 1067, 910, 749, 699 cm^{-1}. ^1H NMR (DMSO-d_6, ppm, δ): 12.8–11.9 (br, COO*H*), 7.3–6.1 (m, Ar—*H*), 4.6–4.5 (br, CH_2N_3), 2.2–2.1 (br, C*H* of polymer backbone), 1.8–1.0 (CH_2 of polymer backbone).

General Preparation of $PTHPA_n$ Polymers 12 and 15

A mixture of *S*-methoxycarbonylphenylmethyl dithiobenzoate (72 mg, 0.24 mmol), AIBN (4.0 mg, 0.02 mmol), and THPA (5.6 g, 35.9 mmol) were degassed by three freeze/pump/thaw cycles, sealed under argon, and heated at 70 °C for 22 h. The viscous reaction mixture was then dissolved in THF (10 mL) and precipitated three times into hexane (200 mL) at *ca.* −70 °C. The resulting pale pink solid, **15**, was dried under vacuum overnight (2.2 g, 39% yield), $M_{n,NMR}$ = 11,800 g/mol, $M_{n,GPC}$ = 11,300 g/mol, M_w/M_n = 1.11. DSC: $(T_g)_{PTHPA}$ = 47 °C.

IR: 3015–2770, 1735, 1442, 1356, 1251, 1211, 1165, 1119, 1036, 1025, 941, 899, 867, 820 cm^{-1}. ^1H NMR ($CDCl_3$, ppm, δ): 6.00–5.89 (C(O)OC*H*CH$_2$), 3.99–3.79 (C(O)OCHC*H*$_2$), 3.70–3.58 (C(O)OCHC*H*$_2$), 2.51–2.15 (br, C*H* of the polymer backbone), 2.03–1.19 (br, meso, and racemo CH_2 of the polymer backbone and 3CH_2 of THP group).

As described for **15** except *S*-propargyloxycarbonylphenylmethyl dithiobenzoate was utilized as the initiator to afford **12** (2.4 g, 41% yield); $M_{n,NMR}$ = 11,000 g/mol, $M_{n,GPC}$ = 11,900 g/mol, M_w/M_n = 1.12. DSC: $(T_g)_{PTHPA}$ = 48 °C.

IR: 3297, 2123, 1739, 1444, 1355, 1251, 1207, 1161, 1117, 1033, 1023, 943, 899, 866, 819 cm^{-1}. ^1H NMR ($CDCl_3$, ppm, δ): 6.05–5.89 (C(O)OC*H*CH$_2$), 3.92–3.80 (C(O)OCHC*H*$_2$), 3.71–3.55 (C(O)OCHC*H*$_2$), 3.14–3.01 (C≡C*H*), 2.51–2.19 (br, C*H* of the polymer backbone), 2.10−1.18 (br, meso, and racemo CH_2 of the polymer backbone and 3CH_2 of THP group).

General Preparation of $PTHPA_n$-b-PS_m Diblock Copolymers, 13 and 16

$PTHPA_{70}$ macroinitiator ($M_{n,NMR}$ = 10,800 g/mol, $M_{n,GPC}$ = 11,300 g/mol, M_w/M_n = 1.11), **15**, was dissolved in St (3.0 g, 29 mmol), and benzene (1.5 mL) and AIBN (1.6 mg, 0.26 mmol) were added. The solution was degassed by three freeze/pump/thaw cycles, sealed under argon, and heated at 70 °C for 10 h. The solidified reaction mixture was then dissolved in THF (20 mL) and precipitated into cold hexane (2 × 800 mL). The precipitate was collected by vacuum filtration and dried overnight *in vacuo* to give the desired block copolymer, **16**, $PTHPA_{70}$-*b*-PS_{130}, as a pale pink solid (2.41 g, 57% yield), $M_{n,NMR}$ = 24,100 g/mol, $M_{n,GPC}$ = 25,200 g/mol, M_w/M_n = 1.16. DSC: $(T_g)_{PTHPA}$ = 47 °C, $(T_g)_{PS}$ = 98 °C.

IR: 3060–2830, 1728, 1601, 1543, 1493, 1259, 1179, 1070, 1028, 965, 906, 804, cm^{-1}. ^1H NMR ($CDCl_3$, ppm, δ): 7.25–6.30 (m, 5Ar—*H*), 6.02–5.94 (C(O)OC*H*CH$_2$), 3.95–3.70 (C(O)OCHC*H*$_2$), 3.68–3.55 (C(O)OCHC*H*$_2$), 2.55–2.18 (br, C*H* of the polymer backbone), 2.08–1.19 (br, meso, and racemo CH_2 of the polymer backbone and 3CH_2 of THP group).

As described for **16** except **12** was utilized as the macroinitiator to afford **13**, HC≡C$PTHPA_{70}$-*b*-PS_{135} (2.31 g, 49% yield); $M_{n,NMR}$ = 25,300 g/mol, $M_{n,GPC}$ = 26,100 g/mol, M_w/M_n = 1.15. DSC: $(T_g)_{PTHPA}$ = 48 °C, $(T_g)_{PS}$ = 103 °C.

IR: 3299, 2119, 1727, 1601, 1543, 1493, 1259, 1179, 1070, 1028, 965, 906, 804, 758, 699 cm^{-1}. ^1H NMR ($CDCl_3$, ppm, δ): 7.22–6.20 (m,

5Ar—*H*), 6.01–5.89 (C(O)OC*H*CH$_2$), 3.97–3.71 (C(O)OCHC*H*$_2$), 3.68–3.55 (C(O)OCHC*H*$_2$), 3.11–3.03 (C≡C*H*), 2.51–2.18 (br, C*H* of the polymer backbone), 2.08-1.19 (br, meso, and racemo C*H*$_2$ of the polymer backbone and 3C*H*$_2$ of THP group).

Preparation of PAA$_n$-b-PS $_m$ Diblock Copolymers, 11 and 14

To a 100-mL, round-bottom flask equipped with a stir bar was added PTHPA$_{70}$-*b*-PS$_{130}$ **16** ($M_{n,GPC}$ = 25,200 g/mol, M_w/M_n = 1.16; 1.0 g, 2.77 mmol of ester groups), followed by tetrahydrofuran (20 mL). The mixture was allowed to stir for 30 min to dissolve the polymer and then deionized water was added (10 mL), followed by glacial acetic acid (40 mL). After the mixture was allowed to stir overnight at RT, the reaction mixture was transferred to presoaked dialysis membrane tubes (MWCO *ca.* 6–8 kDa), and dialysis against deionized water for 4 days. Lyophilization gave **14**, PAA$_{70}$-*b*-PS$_{130}$, as a pale pink solid, (0.65 g, 94% yield). DSC: $(T_g)_{PAA}$ = 134 °C, $(T_g)_{PS}$ = 96 °C.

IR: 3550–2830, 1710, 1493, 1452, 1396, 1249, 1163, 1065, 1024, 864, 841, 759, 699 cm^{-1}. ^{1}H NMR (DMSO-d_6, ppm, δ): 13.1–12.0 (br, COO*H*), 7.6–6.5 (m, 5Ar—*H*), 2.3–1.4 (br, C*H* and C*H*$_2$ of polymer backbone).

As described for **14** except **13** was utilized as the prepolymer to afford **11**, HC≡CPAA$_{70}$-*b*-PS$_{135}$ (0.68 g, 94% yield). DSC: $(T_g)_{PAA}$ = 131 °C, $(T_g)_{PS}$ = 99 °C.

IR: 3296, 2120, 1705, 1493, 1452, 1399, 1249, 1163, 1065, 864, 759, 701, 669 cm^{-1}. ^{1}H NMR (DMSO-d_6, ppm, δ): 13.2–11.9 (br, COO*H*), 7.4–6.1 (m, 5Ar—*H*), 3.1–3.0 (C≡C*H*), 2.3–1.0 (br, C*H*, and C*H*$_2$ of polymer backbone).

Preparation of Alkynyl Chain End-Functionalized Micelle, 8

A round-bottom flask equipped with a stirrer bar was charged with PAA$_{70}$-*b*-PS$_{130}$, **14**, ($M_{n,NMR}$ = 20,800 g/mol) and HC≡CPAA$_{70}$-*b*-PS$_{135}$, **11**, ($M_{n,NMR}$ = 19,900 g/mol) in various ratios, THF (1 mg/mL) was added, and the solution was allowed to stir at RT for 30 min to ensure the mixture was homogenous. Deionized water (500 mL) was added via a metering pump at the rate of 20 mL/h. After all of the water had been added, the bluish micelle solution was transferred to dialysis tubing (MWCO *ca.* 6–8 kDa), and dialyzed against deionized water for 4 days to remove all of the THF. D_h (DLS) = 49 ± 4 nm; D_{av} (TEM): 37 ± 3 nm. Lyophilization gave **8** as a pale pink solid. DSC: $(T_g)_{PAA}$ = 132 °C, $(T_g)_{PS}$ = 100 °C.

IR: 3299, 2121, 1716, 1704, 1657, 1638, 1565, 1442, 1248, 1197, 1053, 780, 702 cm^{-1}.

Preparation of Chain End-Functionalized SCK Nanoparticles, 9 and 17

To a stirred solution of micelle **7** (500 mL, 0.29 mg/mL, 0.50 mmol of acrylic acid) in a round-bottomed flask equipped with a stir bar was added, dropwise over 10 min, a solution of 2,2′-(ethylenedioxy)bis(ethylamine) (0.020 g, 0.13 mmol) in deionized water (5.0 mL). The solution was allowed to stir for 2 h at RT. To this reaction mixture was added dropwise, via a metering pump at the rate of 20 mL/h, a solution of 1-[3′-(dimethylamino)propyl]-3-ethylcarbodiimide methiodide (0.071 g, 0.25 mmol) dissolved in deionized water (100 mL). The reaction mixture was allowed to stir overnight at RT and was then transferred to presoaked dialysis membrane tubes (MWCO *ca.* 6–8 kDa), and dialyzed against deionized water for 4 days to remove small molecule contaminants. Final concentration of solution of **17** was *ca.* 0.28 mg/mL. D_h (DLS) = 44 ± 3 nm; D_{av} (TEM): 34 ± 4 nm; D_{av} (AFM): 104 ± 16 nm; H_{av} (AFM): 4.8 ± 1.2 nm. Lyophilization gave **17** as a white solid. DSC: $(T_g)_{PS}$ = 97 °C.

IR: 3285–2925, 2100, 1715, 1695, 1644, 1562, 1530, 1451, 1248, 1171, 1106, 1066, 761, 694 cm^{-1}.

As described for **17** except **8** was utilized as the micelle to afford **9**: Final concentration of solution of **9** *ca.* 0.28 mg/mL. D_h (DLS) = 43 ± 4 nm; D_{av} (TEM): 32 ± 3 nm; D_{av} (AFM): 117 ± 18 nm; H_{av} (AFM): 2.4 ± 0.4 nm. Lyophilization gave **9** as a white solid. DSC: $(T_g)_{PS}$ = 99 °C.

IR: 3295, 2125, 1714, 1695, 1644, 1569, 1539, 1452, 1257, 1189, 1105, 1056, 756, 699 cm^{-1}.

Click Reaction of Surface Azido-Functionalized SCK Nanoparticle with Fluorescein Dye, 18

A 50 mL, round-bottom flask was charged with a magnetic stir bar, alkynyl fluorescent dye, **19** (0.0033 g, 0.0056 mmol),[87,88] $CuSO_4 \cdot 5H_2O$ (0.0035 g, 0.014 mmol), H_2O (20 mL), and a freshly prepared 5 wt % aqueous solution of sodium ascorbic acid (0.057 mL, 0.007 mmol). The mixture was allowed to stir at RT for 30 min and was then added to a 500 mL, round-bottom flask that was charged with the aqueous nanoparticle solution,

17, (600 mL, 0.0028 mmol of azido groups) and a magnetic stir bar. The reaction mixture was allowed to stir for 2 days at RT and was then transferred to presoaked dialysis membrane tubes (MWCO *ca.* 6–8 kDa), and dialyzed against 50 mM sodium phosphate, 1.0 M sodium chloride, pH 7.3, for 10 days to remove excess dye and copper catalyst. To remove any traces of residual dye the nanoparticle solutions were subjected to a secondary dialysis step using a 10 mL stirred cell (Stirred Ultrafiltration Cell, Millipore, 10 kDa MWCO membrane) and flushed three times with Nanopure water (*ca.* 7 mL). D_h (DLS) = 34 ± 4 nm; D_{av} (TEM): 37 ± 5 nm; D_{av} (AFM): 126 ± 14 nm; H_{av} (AFM): 8.9 ± 2.2 nm. Lyophilization gave **18** as a pale yellow solid. DSC: $(T_g)_{PS}$ = 99 °C.

These results are based upon work supported by the National Science Foundation under the Nanoscale Interdisciplinary Research Team (NIRT) program Grant number 0210247, MRSEC program (UCSB MRL, DMR-0520415), CHE-0514031, and DMR-0451490, and by the National Institutes of Health as a Program of Excellence in Nanotechnology (1 U01 HL080729-01). R.K. O'Reilly was partially supported by a Research Fellowship from the Royal Commission of the Exhibition of 1851. M.J. Joralemon was supported by a Chemistry-Biology Interface Program Fellowship under an NIH Training Grant No. NIHNRSA 5-T32-GM08785-0. G. Michael Veith, Department of Biology, Washington University, is gratefully acknowledged for TEM analysis. Jeffery L. Turner is thanked for schematic drawings of SCK nanoparticles.

REFERENCES AND NOTES

1. Hawker, C. J.; Wooley, K. L. Science 2005, 309, 1200.
2. Zhang, L. F.; Yu, K.; Eisenberg, A. Science 1996, 272, 1777.
3. Discher, D. E.; Eisenberg, A. Science 2002, 297, 967.
4. Matejicek, P.; Uhlik, F.; Limpouchova, Z.; Prochazka, K.; Tuzar, Z.; Webber, S. E. Macromolecules 2002, 35, 9487.
5. Zhang, L. F.; Eisenberg, A. J Am Chem Soc 1996, 118, 3168.
6. Moses, M. A.; Brem, H.; Langer, R. Cancer Cell 2003, 4, 337.
7. Thurmond, K. B., II; Remsen, E. E.; Kowalewski, T.; Wooley, K. L. Nucleic Acids Res 1999, 27, 2966.
8. Zhang, Q.; Remsen, E. E.; Wooley, K. L. J Am Chem Soc 2000, 122, 3642.
9. Webber, S. E. J Phys Chem B 1998, 102, 2618.
10. Ma, Y. G.; Kolotuchin, S. V.; Zimmerman, S. C. J Am Chem Soc 2002, 124, 13757.
11. Abraham, S.; Ha, C.-S.; Kim, I. J Polym Sci Part A: Polym Chem 2005, 43, 6367.
12. Jia, Z.; Zhou, Y.; Yan, D. J Polym Sci Part A: Polym Chem 2005, 43, 6534.
13. Lodge, T. P. Macromol Chem Phys 2003, 204, 265.
14. Murthy, K. S.; Ma, Q. G.; Remsen, E. E.; Kowalewski, T.; Wooley, K. L. J Mater Chem 2003, 13, 2785.
15. Gillies, E. R.; Fréchet, J. M. J. Chem Commun 2003, 1640.
16. Wooley, K. L. Chem—Eur J 1997, 3, 1397.
17. (a) Thurmond, K. B., II; Kowalewski, T.; Wooley, K. L. J Am Chem Soc 1996, 118, 7239; (b) Thurmond, K. B., II; Kowalewski, T.; Wooley, K. L. J Am Chem Soc 1997, 119, 6656.
18. (a) Aubrecht, K. B.; Grubbs, R. B. J Polym Sci Part A: Polym Chem 2005, 43, 5156; (b) Liu, B.; Perrier, S. J Polym Sci Part A: Polym Chem 2005, 43, 3643; (c) Chang, Y.; Powell, E. S.; Allcock, H. R. J Polym Sci Part A: Polym Chem 2005, 43, 2912.
19. Huang, H.; Remsen, E. E.; Wooley, K. L. Chem Commun 1998, 1415.
20. Ding, J. F.; Liu, G. J. Macromolecules 1998, 31, 6554.
21. Bütün, V.; Billingham, N. C.; Armes, S. P. J Am Chem Soc 1998, 120, 12135.
22. Cao, L.; Manners, I.; Winnik, M. A. Macromolecules 2001, 34, 3353.
23. Sanji, T.; Nakatsuka, Y.; Kitayama, F.; Sakurai, H. Chem Commun 1999, 2201.
24. (a) Choucair, A.; Lavigueur, C.; Eisenberg, A.; Langmuir 2004, 20, 3894; (b) Ayres, L.; Hans, P.; Adams, J.; Löwik, D. W. P. M.; van Hest, J. C. M. J Polym Sci Part A: Polym Chem 2005, 43, 6355.
25. Terreau, O.; Luo, L. B.; Eisenberg, A. Langmuir 2003, 19, 5601.
26. (a) Loppinet, B.; Sigel, R.; Larsen, A.; Fytas, G.; Vlassopoulos, D.; Liu, G. Langmuir 2000, 16, 6480; (b) Matsumoto, K.; Matsuoka, H. J Polym Sci Part A: Polym Chem 2005, 43, 3778.
27. Henselwood, F.; Liu, G. J. Macromolecules 1997, 30, 488.
28. Discher, B. M.; Won, Y. Y.; Ege, D. S.; Lee, J. C. M.; Bates, F. S.; Discher, D. E.; Hammer, D. A. Science 1999, 284, 1143.
29. Huang, H. Y.; Kowalewski, T.; Remsen, E. E.; Gertzmann, R.; Wooley, K. L. J Am Chem Soc 1997, 119, 11653.
30. Ma, Q. G.; Remsen, E. E.; Kowalewski, T.; Wooley, K. L. J Am Chem Soc 2001, 123, 4627.
31. Wooley, K. L. J Polym Sci Part A: Poly Chem 2000, 38, 1397.
32. Ding, J. F.; Liu, G. J. Macromolecules 1999, 32, 8413.
33. Ma, Q. G.; Remsen, E. E.; Kowalewski, T.; Schaefer, J. Wooley, K. L. Nano Lett 2001, 1, 651.
34. Butun, V.; Lowe, A. B.; Billingham, N. C.; Armes, S. P. J Am Chem Soc 1999, 121, 4288.
35. Liu, S.; Armes, S. P. Langmuir 2003, 19, 4432.

36. Kao, H. M.; O'Connor, R. D.; Mehta, A. K.; Huang, H. Y.; Poliks, B.; Wooley, K. L.; Schaefer, J. Macromolecules 2001, 34, 544.
37. Baugher, A. H.; Goetz, J. M.; McDowell, L. M.; Huang, H. Y.; Wooley, K. L.; Schaefer, J. Biophys J 1998, 75, 2574.
38. Huang, H. Y.; Wooley, K. L.; Schaefer, J. Macromolecules 2001, 34, 547.
39. Turner, J. L.; Wooley, K. L. Nano Lett 2004, 4, 683.
40. Clark, C. G.; Wooley, K. L. Curr Opin Colloid Interface Sci 1999, 4, 122.
41. Huang, H. Y.; Remsen, E. E.; Kowalewski, T.; Wooley, K. L. J Am Chem Soc 1999, 121, 3805.
42. Sun, X. K.; Rossin, R.; Turner, J. L.; Becker, M. L.; Joralemon, M. J.; Welch, M. J.; Wooley, K. L. Biomacromolecules 2005, 6, 2541.
43. Niemeyer, C. M. Angew Chem Int Ed 2001, 40, 4128.
44. Narain, R.; Armes, S. P. Macromolecules 2003, 36, 4675.
45. Sarikaya, M.; Tamerler, C.; Jen, A. K. Y.; Schulten, K.; Baneyx, F. Nat Mater 2003, 2, 577.
46. Berry, C. C.; Curtis, A. S. G. J Phys D: Appl Phys 2003, 36, R198.
47. Kakizawa, Y.; Kataoka, K. Adv Drug Delivery Rev 2002, 54, 203.
48. Kataoka, K.; Harada, A.; Nagasaki, Y. Adv Drug Delivery Rev 2001, 47, 113.
49. Langer, R. Science 2001, 293, 58.
50. Lynn, D. M.; Amiji, M. M.; Langer, R. Angew Chem Int Ed 2001, 40, 1707.
51. Cao, Y. W. C.; Jin, R. C.; Mirkin, C. A. Science 2002, 297, 1536.
52. Taton, T. A.; Mirkin, C. A.; Letsinger, R. L. Science 2000, 289, 1757.
53. Torchilin, V. P. Cell Mol Life Sci 2004, 61, 2549.
54. Rosler, A.; Vandermeulen, G. W. M.; Klok, H.-A. Adv Drug Deliv Rev 2001, 53, 95.
55. Joralemon, M. J.; Murthy, K. S.; Remsen, E. E.; Becker, M. L.; Wooley, K. L. Biomacromolecules 2004, 5, 903.
56. Pan, D.; Turner, J. L.; Wooley, K. L. Chem Commun 2003, 2400.
57. Licciardi, M.; Tang, Y.; Billingham, N. C.; Armes, S. P. Biomacromolecules 2005, 6, 1085.
58. Becker, M. L.; Remsen, E. E.; Pan, D.; Wooley, K. L. Bioconjugate Chem 2004, 15, 699.
59. Becker, M. L.; Liu, J. Q.; Wooley, K. L. Biomacromolecules 2005, 6, 220.
60. Pan, D. J.; Turner, J. L.; Wooley, K. L. Macromolecules 2004, 37, 7109.
61. Joralemon, M. J.; Smith, N. L.; Holowka, D.; Baird, B.; Wooley, K. L. Bioconjugate Chem 2005, 16, 1246.
62. Qi, K.; Ma, Q. G.; Remsen, E. E.; Clark, C. G.; Wooley, K. L. J Am Chem Soc 2004, 126, 6599.
63. Jia, Y. M.; Gray, G. M.; Hay, J. N.; Li, Y. T.; Unali, G. F.; Baines, F. L.; Armes, S. P. J Mater Chem 2005, 15, 2202.
64. Salvage, J. P.; Rose, S. F.; Phillips, G. J.; Hanlon, G. W.; Lloyd, A. W.; Ma, I. Y.; Armes, S. P.; Billingham, N. C.; Lewis, A. L. J Controlled Release 2005, 104, 259.
65. Turner, J. L.; Pan, D. P. J.; Plummer, R.; Chen, Z. Y.; Whittaker, A. K.; Wooley, K. L. Adv Funct Mater 2005, 15, 1248.
66. Turner, J. L.; Becker, M. L.; Li, X.; Taylor, J.-S.; Wooley, K. L. Soft Matter 2005, 1, 69.
67. Becker, M. L.; Liu, J. Q.; Wooley, K. L. Chem Commun 2003, 802.
68. Liu, J. Q.; Zhang, Q.; Remsen, E. E.; Wooley, K. L. Biomacromolecules 2001, 2, 362.
69. Rossin, R.; Pan, D. P. J.; Qi, K.; Turner, J. L.; Sun, X. K.; Wooley, K. L.; Welch, M. J. J Nucl Med 2005, 46, 1210.
70. Rostovtsev, V. V.; Green, L. G.; Fokin, V. V.; Sharpless, K. B. Angew Chem Int Ed 2002, 41, 2596.
71. (a) Mocharla, V. P.; Colasson, B.; Lee, L. V.; Roper, S.; Sharpless, K. B.; Wong, C. H.; Kolb, H. C. Angew Chem Int Ed Engl 2005, 44, 116; (b) Díaz, D. D.; Punna, S.; Holzer, P.; McPherson, A. K.; Sharpless, K. B.; Fokin, V. V.; Finn, M. G. J Polym Sci Part A: Polym Chem 2004, 42, 4392.
72. Joralemon, M. J.; O'Reilly, R. K.; Matson, J. B.; Nugent, A. K.; Hawker, C. J.; Wooley, K. L. Macromolecules 2005, 38, 5436.
73. Suh, B.-C.; Jeon, H.; Posner, G. H.; Silverman, S. M. Tetrahedron Lett 2004, 45, 4623.
74. Lee, J. K.; Chi, Y. S.; Choi, I. S. Langmuir 2004, 20, 3844.
75. Tsarevsky, N. V.; Bernaerts, K. V.; Dufour, B.; Du Prez, F. E.; Matyjaszewski, K. Macromolecules 2004, 37, 9308.
76. Tsarevsky, N. V.; Sumerlin, B. S.; Matyjaszewski, K. Macromolecules 2005, 38, 3558.
77. Mantovani, G.; Ladmiral, V.; Tao, L.; Haddleton, D. M. Chem Commun 2005, 2089.
78. Parrish, B.; Breitenkamp, R. B.; Emrick, T. J Am Chem Soc 2005, 127, 7404.
79. Opsteen, J. A.; van Hest, J. C. M. Chem Commun 2005, 57.
80. Malkoch, M.; Schleicher, K.; Drockenmuller, E.; Hawker, C. J.; Russell, T. P.; Wu, P.; Fokin, V. V. Macromolecules 2005, 38, 3663.
81. (a) O'Reilly, R. K.; Joralemon, M. J.; Hawker, C. J.; Wooley, K. L. Chem Mater 2005, 17, 5976; (b) Wegrzyn, J. K.; Stephan, T.; Lau, R.; Grubbs, R. B. J Polym Sci Part A: Polym Chem 2005, 43, 2977; (c) Yin, M.; Krause, T.; Messerschmidt, M.; Habicher, W. D.; Voit, B. J Polym Sci Part A: Polym Chem 2005, 43, 1873.
82. Benoit, D.; Chaplinski, V.; Braslau, R.; Hawker, C. J. J Am Chem Soc 1999, 121, 3904.
83. Hertler, W. R.; Sogah, D. Y.; Raymond, F. A.; Bauer, R. D.; Chang, C. T.; Taylor, G. N.; Stillwagon, L. E. Makromol Chem Macromol Symp 1992, 64, 137.

84. (a) Chiefari, J.; Chong, Y. K.; Ercole, F.; Krstina, J.; Jeffery, J.; Le, T. P. T.; Mayadunne, R. T. A.; Meijs, G. F.; Moad, C. L.; Moad, G.; Rizzardo, E.; Thang, S. H. Macromolecules 1998, 31, 5559; (b) Nguyen, M. N.; Bressy, C.; Margaillan, A. J Polym Sci Part A: Polym Chem 2005, 43, 5680; (c) Perrier, S.; Takolpuckdee, P. J Polym Sci Part A: Polym Chem 2005, 43, 5347; (d) Goh, Y.-K.; Whittaker, M. R.; Monteiro, M. J. J Polym Sci Part A: Polym Chem 2005, 43, 5232; (e) Monteiro, M. J. J Polym Sci Part A: Polym Chem 2005, 43, 3189; (f) Li, C.; Benicewicz, B. C. J Polym Sci Part A: Polym Chem 2005, 43, 1535; (g) Drockenmuller, E.; Li, L. Y. T.; Ryu, D. Y.; Harth, E.; Russell, T. P.; Kim, H.-C.; Hawker, C. J. J Polym Sci Part A: Polym Chem 2005, 43, 1028.
85. Lee, W.; Malkoch, M.; Drockenmuller, E.; Hawker, C. J. J Polym Sci Part A: Polym Chem 2006, submitted for publication.
86. O'Reilly, R. K.; Joralemon, M. J.; Hawker, C. J.; Wooley, K. L. Chem—Eur J 2006, Early View.
87. Crisp, G. T.; Gore, J. Tetrahedron 1997, 53, 1505.
88. Deiters, A.; Cropp, T. A.; Mukherji, M.; Chin, J. W.; Anderson, J. C.; Schultz, P. G. J Am Chem Soc 2003, 125, 11782.
89. Perrier, S.; Takolpuckdee, P.; Westwood, J.; Lewis, D. M. Macromolecules 2004, 37, 2709.
90. Bräse, S.; Gil, C.; Knepper, K.; Zimmerman, V. Angew Chem Int Ed 2005, 44, 5188.
91. To 9 separate aliquots of a nanoparticle solution of **18** (concentration of 0.28 mg of nanoparticles per mL of solvent) were added appropriate amounts of acid or base to afford nanoparticle solutions with identical concentrations of **18** and with pH's ranging from 3.8 to 9.5. The free dye solutions were prepared with the same molar concentration of fluorescein units as the solutions of **18**.